The Effect of the Angle of Inclination on the Efficiency in a Medium-Temperature Flat Plate Solar Collector

Orlando Montoya-Marquez and José Jasson Flores-Prieto *

National Center of Research and Develop of Technology-TecNM-SEP, Interior Internado Palmira s/n, Cuernavaca 62490, Morelos, Mexico; orlando_m_marquez@hotmail.com

* Correspondence: jasson@cenidet.edu.mx; Tel.: +52-777-362-7770 (ext. 1302); Fax: +52-777-362-7795

Abstract: In this experimental work, the effects of the inclination angle β and the $(T_i - T_a)/G$ on the efficiency and the U_L-value were investigated on a medium-temperature flat plate solar collector. The experiments were based on steady-state energy balance, by heat flow calorimetry at indoor conditions and considering the standard American National Standard Institute/American Society of Heating Refrigerating and Air Conditioning Engineers (ANSI/ASHRAE) 93-2010. The solar radiation was emulated by the Joule effect using a proportional integral derivative (PID) control considering two conditions of the absorber temperature, Case 1: $(T_o - T_i) > 0$, and Case 2: $(T_o - T_i) = 0$. The inclination angles were 0°–90° and the $(T_i - T_a)/G$ were 0.044–0.083 m²·°C/W and 0.124–0.235 for Case 1 and Case 2, respectively. The variations of β and $(T_i - T_a)/G$ cause efficiency changes up to 0.37–0.45 (21.6%) and 0.31–0.45 (45.0%), respectively, for Case 1. Also, the $U_L(β)$ reached changes up to 10.1–12.0 W/m²·°C (19.2%) and 8.4–12.0 W/m²·°C (41.7%), respectively, for Case 1. The most significant changes of $U_L(β)/U_L(90°)$ vs. β were 8.0% at the horizontal position for Case 1, while for Case 2, the maximum change was 1.8% only. Therefore, the changes of the inclination angle cause significant variations of the convective flow patterns within the collector, which leads to considerable variation of the collector efficiency and its U_L value.

1. Introduction

The solar heating systems for industrial applications have a great potential to reduce the demand for conventional energy. This technology could supply 406 GW$_{th}$ [1]. Currently, the world's solar heating by flat plate collectors is about 83.9 GW$_{th}$ [1]. The glazing flat plate solar collectors are one of the most used devices for solar heating, due to being able to reach more than the desired temperatures, collecting direct and diffuse radiation at a lower cost due to their construction and operation simplicity [2]. The characterization and simulation have improved the commercialization and their applications in most heating processes. Therefore, anything focusing on better characterization of solar collectors has been welcomed for the solar heating industry because that allows reducing estimation uncertainty, in order to have a more accurate picture of their performance.

Most of the previous reports show theoretical and experimental models to determine the thermal efficiency of solar collectors, in terms of the transmittance-absorbance factor τα, the overall heat transfer U_L and the heat removal factor F_R [3]. These models usually consider the collector tilt angle with respect to the normal axis of the surface, mainly taking into account the variations with respect to the east-west axis, as a common daily variation. The ANSI/ASHRAE 93-2010 [4] and International Standard Organization (ISO) 9806:2013 [5] show methods to determine the influence of the incidence

angle which only amend the first coefficient of the efficiency curve ($F_R\tau\alpha$). Then the tilt angle with respect to the North-South (N-S) horizontal axis is currently taken into account to determine a constant value of U_L, as this varies only during the few days of the collector's test [4,5]. Currently, the effect of the change of the inclination angle is included in the third coefficient of the collector efficiency curve along with many other effects, as well as in the Incident Angle Modifier (IAM) to fit the first coefficient [4].

Among the research models, previous works have also proposed an overall heat loss coefficient and experimental generalized correlations as complements to determine the solar collector's efficiency [6–9]. However, these proposed models generally use a fixed inclination with respect to the N-S horizontal axis, according to the latitude of the evaluation place [10,11], thereby disregarding the fact that the second and third coefficients of the efficiency curve are functions of the U_L. This latter is, in turn, dependent on the collector's inclination, due to the changes of the convective flow pattern of the confined fluid between the absorber and the cover of the collector. To date, the determinations of U_L as a function of the collector inclination β have been weakly studied, separating the effect of the confined fluid and the incidence solar radiation, as well as the effect of working at higher differences of temperature ($T_p - T_a$), as is the case for medium-temperature solar collectors for industrial processes.

Ozoe et al. [12,13] and Alvarado et al. [14], among others, have shown the changes of the flow pattern with the collector inclination with respect to the horizontal position. However, lower ($T_p - T_a$) and the collector's inclination as used at characterization place do not make a big difference. Bava and Furbo [15] carried out a parametric experimental study varying the collector type, the solar collector fluid, the volume flow rate and the collector inclination to determine the performance in terms of efficiency. They found that the flat plate collector is most commonly used at inclination angles of 30°, 45° and 60° of, in a range of 20–100 °C. On the other hand, Sabatelli et al. [16] developed a test method to evaluate the efficiency uncertainty for the ISO 9806/1 standard. Beikircher et al. [17] developed a procedure to determine the collector thermal efficiency based on heat loss measurements without insulation. Bava and Furbo [15] found that the most important parameter in the sensibility of the U_L is the inclination angle, which can represent 5%–8% of U_L change. Thus, the use of a higher temperature between the absorber plate and the glazing cover, as well as the increase of the movement of products around the world, causes the effect of inclination on the collector's efficiency, and more careful studies are required.

Therefore, a study of the effects of the inclination angle on the efficiency and the overall heat transfer coefficient was proposed and investigated in a glazing flat plate collector under inclinations from horizontal to vertical, varying ($T_i - T_a$)/G for working conditions of some of the medium-temperature solar collectors.

2. Materials and Methods
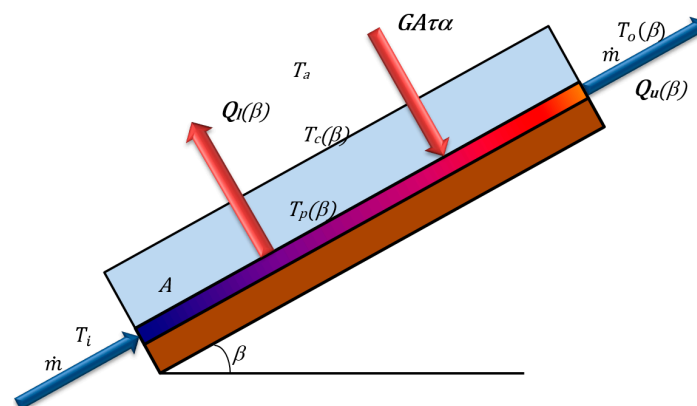
2.1. Sampling

Figures 1 and 2 show a sketch and a picture of the flat plate solar collector respectively. The sample is 2.00 m² (1.00 m × 2.00 m) of gross collector area, with an aspect ratio of 40. The solar collector has a couple header tubes and five raising finned tubes, all of them of cooper, joined by tin-lead solder. The working fluid was water-glycol 10%–90%, considering variable heat capacity as function of the temperature [18]. The surface of absorber plate was covered with black matte paint with absorptance of 0.94. The solar transmittance of the glazing was 0.86. The spectral absorptance and transmittance were obtained according to CIE 130-1998 [19], using a spectrophotometer Shimadzu UV-3100, (Shimadzu Corpotation, Nakagyo-ku, Kyoto, Japan), in the range of 300–2500 nm, every 2.0 nm with ±0.1% of photometric uncertainty and 1.0% of wavelength uncertainty. The absorptance was obtained by normalizing the measured spectral absorptance according ISO 9050-2003 [20]. Table 1 shows the solar collector construction characteristics.

Table 1. Construction specifications of the solar collector.

Parameter	Dimension	Units
Aspect ratio of enclosure	40	-
Copper absorber area	1.95×0.95	m
Fin width	0.19	m
Diameter of heaters	0.0381	m
Diameter of reassign tubes	0.0127	m
Fin thickness	0.5	mm
Absortance	0.94	-
Fiber glass insulation	0.0254	m
Cover of glass shit	3.0	mm

2.2. Experimental Design

The experimental design allows determining the U_L and collector efficiency η, under inclinations from horizontal to vertical, at a range of $(T_i - T_a)/G$. All of the rest variables involved in the experiment were considered without significant variations. Once the experiment works emulating the solar heating, part of the supplied energy heats the working fluid Q_u, and the rest is transferred to the ambient as heat losses $Q_l(\beta)$, both of them also dependent from the β and $(T_i - T_a)/G$. The $U_L(\beta,(T_i - T_a)/G)$ and $\eta(\beta,(T_i - T_a)/G)$ are determined by flow calorimetry, based on steady-state energy balance according Figure 1, at indoor controlled conditions. Constant solar heating at $(T_o - T_i) > 0$ and isothermal absorber plate at $(T_o - T_i) = 0$ are considered in the study for comparison, looking for achieve suitable experimental uncertainty.

Figure 1. Physical model.

The incoming heat flux is GA, which is fixed and is not considered function of β. The outlet heat is the sum of the $Q_u(\beta)$ plus the heat loss flux $Q_l(\beta)$. The following considerations are taken in to account in the experiment: (a) steady state; (b) constant surrounding temperature and emissivity; (c) constant radiative exchange; (d) linear variation of C_p with the temperature; and (e) the mean plate temperature, $T_p(\beta)$ is considered as the average temperature between outlet and inlet temperature $(T_o(\beta) - T_i)/2$.

Throughout each test once the absorber plate works, it heats the working fluid that flows through the raising tubes. Part of supplied energy heats the working fluid and the rest is transferred to the ambient as heat losses, both of them dependent from the β and $(T_i - T_a)/G$. At indoor conditions, the solar heating is emulated by Joule effect and proportional integral derivative (PID) control, using electrical heater, making possible to replace $(T_i - T_a)/G$ by $(T_i - T_a)/(VI/A\tau\alpha)$, to achieve better experimental uncertainty, thus the solar heating is given by Equation (1).

$$GA = \frac{VI}{\tau\alpha} \tag{1}$$

where τ and α are the glazing solar transmittance and the solar absorptance of the absorber respectively, and *V* and *I* are the electrical voltage and current respectively. Considering the above, due to the convective flow pattern varies with the tilt angle then the overall heat transfer coefficient in terms of β is calculated by:

$$U_L(\beta) = \frac{VI - Q_u(\beta)}{A\left[T_p(\beta) - T_a\right]} \tag{2}$$

where the useful energy is $Q_u(\beta) = \int_{t_1}^{t_2} \dot{m} C_p (T_o(\beta) - T_i) dt$ and the $Q_l(\beta) = A U_L(\beta) \left[T_p(\beta) - T_a\right]$. And then, the collector efficiency, according ANSI/ASHRAE 93-2010, is given by:

$$\eta(\beta) = \frac{Q_u(\beta)}{\left(\frac{VI}{A\tau\alpha}\right)} \tag{3}$$

2.3. Experimental Setup

The heating of the absorber is homogenously distributed by means of the electrical heater and remains almost constant over each test. The experimental setup is sketched in Figure 2.
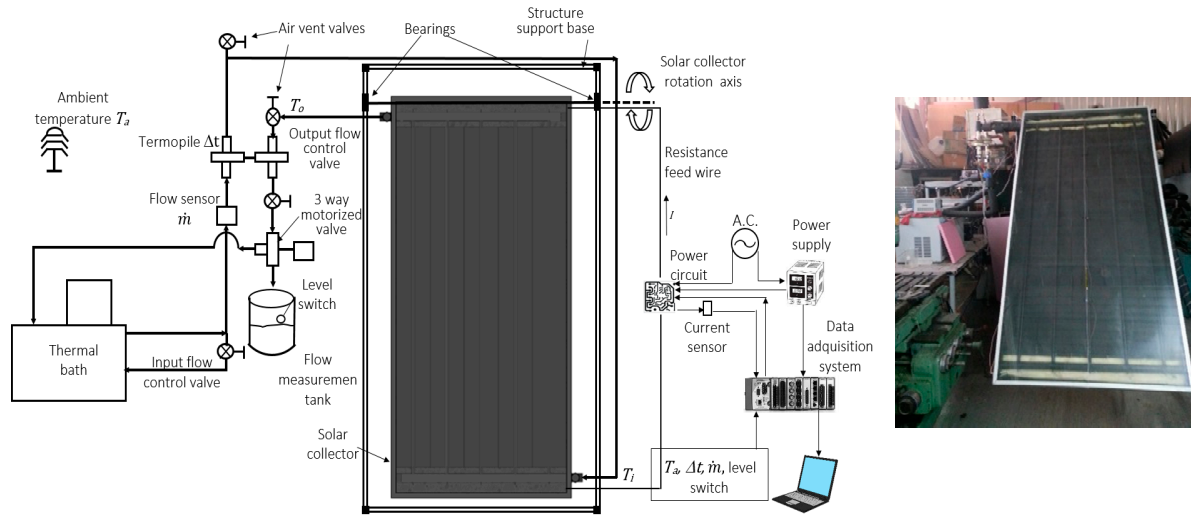

Figure 2. Experimental Setup.

According the heating of the absorber two cases were considered. The Case 1 ($(T_o - T_i) > 0$, $Q_u(\beta) \geq 0$): with considerable profile temperature in the raising tubes, also called non-isothermal absorber plate, which allows to achieve the U_L and the collector efficiency. The Case 2 ($(T_o - T_i) = 0$), $Q_u(\beta) = 0$): also called isothermal absorber plate, which allows to achieve the U_L only. In the Case 1, the *GA* is set to a specified value, therefore $(T_o - T_i)$ and $(T_p - T_a)$ are the output variables. In the Case 2, the $(T_o - T_i)$ are controlled close to zero by adjusting the *VI*, thus $(T_p - T_a)$ is the output variables only.

As is shown in Figure 2, the experimental set up allows mounting the sample with variable angle β at 0°, 30°, 45°, 60° and 90°, with uncertainty of ±0.1°. The $(T_i - T_a)/G$ are fixed at series of specified steps, by adjusting T_i and *VI* in the range of part of low and medium temperature solar collectors (0.044–0.084). The electrical heater supplied up to a maximum of 2000 W, with an uncertainty of ±5 W.

The temperature differentials $(T_o - T_i)$ and $(T_i - T_a)$ were measured using a type *T* thermocouple, 32 gauge wires, with an uncertainty of ±0.1 °C. A thermal bath supplied 10%–90% water-glycol mixture as working fluid, with an uncertainty of ±0.01 °C. The mass flow rate was 0.016 kg/s [15,21]; it was monitored with a turbine-flowmeter, with an uncertainty of 3%, and was also verified by weighing the water-glycol mixture, at specified time steps during the experimental campaign.

The experimental indoor condition allows to keep uniform surrounding temperature, surrounding emissivity, as well as to run the experiments with non-considerable changes of solar heating, ambient temperature, surrounding temperature and wind velocity. The 10%–90% water-glycol mixture allows minimizing adverse boiling effects.

A programmable Field Programmable Gate Array, NI-CompactRIO, 9022 (National Instruments, Austin, TX, USA), 32 bits data acquisition and Lab-VIEW software 2012 (National Instruments, Austin, TX, USA) were used to monitor, recorded and calculate the experimental variables at time steps of one second. During experiments, the steady state was verified by monitoring experimental data without considerable changes at each 30 min. Each data point corresponds to an average of over 1800 measurements, taken during a 30 min period. The test was made by triplicate for comparison.

3. Effect of the Parameters

The experiment focused on the behavior of the overall heat transfer and its effect on the collector's efficiency as a function of the inclination angle and $(T_i - T_a)/G$, emphasizing that $G \neq f(\beta)$ and minimizing the effect of the changes of the rest of the variables. Three sets of 20 experiments were carried out for this purpose. The U_L was studied at β (0°, 30°, 45°, 60° and 90°) and $(T_i - T_a)/G$ at (0.044, 0.056, 0.070, 0.083, 0.124, 0.140, 0.160, 0.195 and 0.235). The efficiency was the same for range β and at $(T_i - T_a)/G$ of (0.044, 0.056, 0.069, 0.083). Case 1 allows the study of the U_L and efficiency at $(T_o - T_i) > 0$, $(Q_u(\beta) > 0)$; the $(T_i - T_a)/G$ and T_p were 0.044, 66.8:0.056, 76.1:0.69, 85.3:0.82, 94.4, respectively. Case 2 allows the study of the U_L only at $(T_o - T_i) = 0$, $(Q_u(\beta) = 0)$; the $(T_i - T_a)/G$ and T_p were 0.235, 60:0.195, 70.0:0.160, 80:0.140, 90:0.124, 100, respectively. Table 2 shows the experimental conditions for the two cases.

Table 2. Experimental conditions for the two study cases.

Parameter	Units	Case 1	Case 2
β	grades	0, 30, 45, 60, 90	0, 30, 45, 60, 90
$(T_o - T_i)$	°C	>0	=0
$Q_u(\beta)$	W	>0	=0
VI	W	constant	Adjustable
$(T_i - T_a)/G$	(m²·°C/W)	0.044, 0.056, 0.070, 0.083	0.124, 0.140, 0.160, 0.195, 0.235
T_i	°C	60.0, 70.0, 80.0, 90.0	60, 70, 80, 90, 100
T_p	°C	66.8, 76.1, 85.3, 94.4	60, 70, 80, 90, 100
$\dot{m}$	kg/s	0.016	0.016

3.1. U_L vs. β and $(T_i - T_a)/G$

3.1.1. Case 1: $(T_o - T_i) > 0$, $(Q_u(\beta) > 0)$

Figure 3 shows U_L vs. β and $(T_i - T_a)/G$ with its corresponding average of T_p. The experimental uncertainty of U_L was ±0.25 W/m²·°C [22]. The T_i was increased to increase the value of T_p and then $(T_i - T_a)/G$ increased as well. It can be observed that the Q_u decreased slower than the increase of $(T_p - T_a)$, causing a U_L value reduction with the increase of T_p. As expected, according Equation (3), the results show that the energy loss $(VI - Q_u)$ increases as $(T_p - T_a)$ increases, while Q_u slowly decreases and VI remains constant. Thus, the U_L decrease due to the Q_u decrease is slower than the increase of $(T_p - T_a)$, causing the U_L value reduction with the increase of T_p.

As seen, $U_L(\beta)$ can achieve a reduction up to 12–10.1 W/m²·°C (19.2%), increasing the inclination angle from 0° to 90° at a constant $(T_i - T_a)/G$ of 0.44. At a constant β, the decreasing rate of the U_L was accentuated at lower values of $(T_i - T_a)/G$. The U_L can change up to 12.0–8.4 W/m²·°C (41.7%), at 0.0° of inclination, into the range we studied of the $(T_i - T_a)/G$. A critical angle was found between 30° and 45° of inclination for each case of $(T_i - T_a)/G$.

The $U_L(\beta)/U_L(90°)$ vs. β correlation for the four different values of $(T_i - T_a)/G$ at $Q_u(\beta) > 0$ is shown in Figure 4. As seen, changing β from 90° to 0°, a significant growth of $U_L(\beta)/U_L(90°)$ ranging from 1.12 to 1.21 (8.0%) was reached at β = 0. The critical angle was also found between 30° and 45° of inclination, which is similar for all the values of the $(T_i - T_a)/G$, while the variation between 0°–30° and 45°–90° seems to be almost linear behavior.
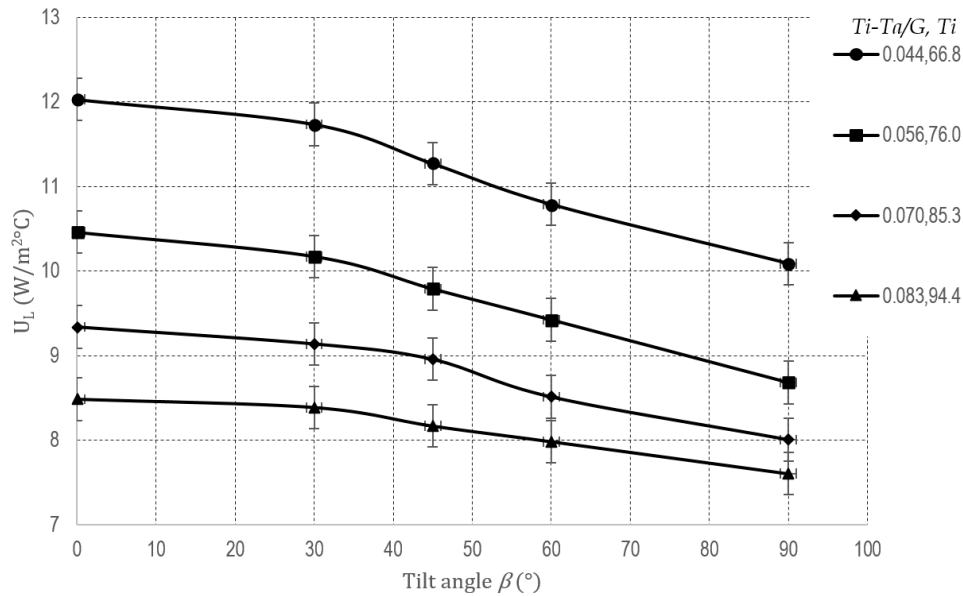

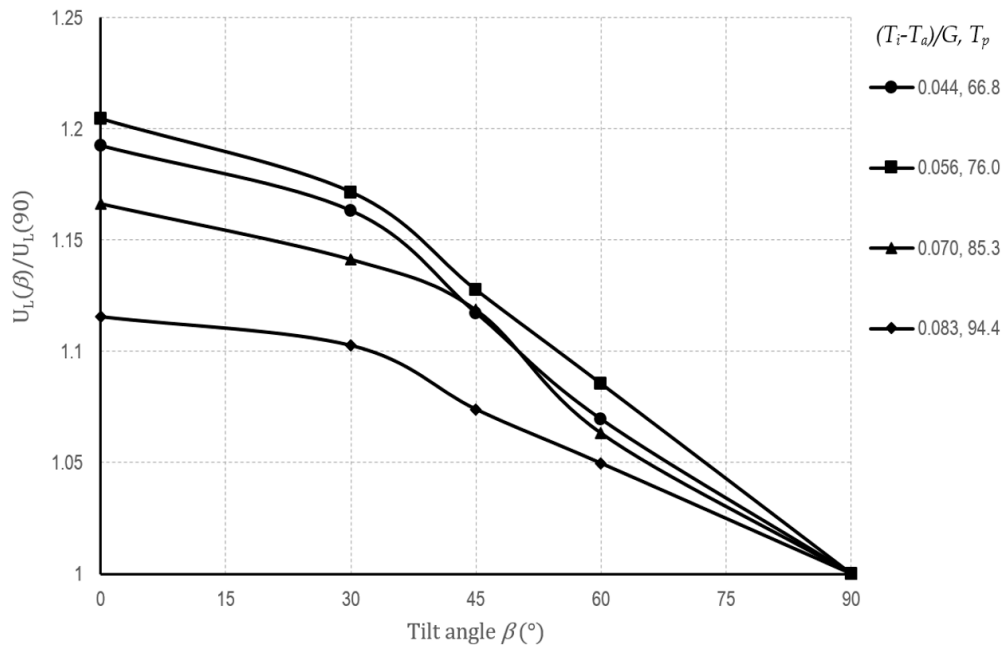**Figure 3.** U_L vs. β, for variable $(T_i - T_a)/G$ at its corresponding T_p, at $Q_u(\beta) > 0$.

Figure 4. $U_L(\beta)/U_L(90°)$ vs. β and $(T_i - T_a)/G$, for Case 1, at $Q_u(\beta) > 0$.

3.1.2. Case 2: $(T_o - T_i) = 0$, $(Q_u(\beta) = 0)$

Figure 5 shows U_L vs. β and $(T_i - T_a)/G$ at its corresponding average of T_p. The experimental uncertainty was only ±0.07 W/m²·°C on average, 247% less than in Case 1. The most important reduction of $U_L(\beta)$ was for lower values of $(T_i - T_a)/G$, from 8.42 to 7.63 W/m²·°C (10.4%), increasing the inclination angle from 0° to 90° at a constant $(T_i - T_a)/G$ of 0.124. As seen in Figures 3 and 5, there

is higher linearity at $(T_o - T_i) = 0$ than when $(T_o - T_i) > 0$, which can be due to the even and uneven surface temperature, which causes a transition flow within the cavity.

Figure 6 shows $U_L(\beta)/U_L(90°)$ vs. β, which ranges from 1.09 to 1.11 only. The $U_L(0)$ could only be increased up to 1.8% of the value of $U_L(90)$, from the highest to lowest values of $(T_i - T_a)/G$ at β = 0.

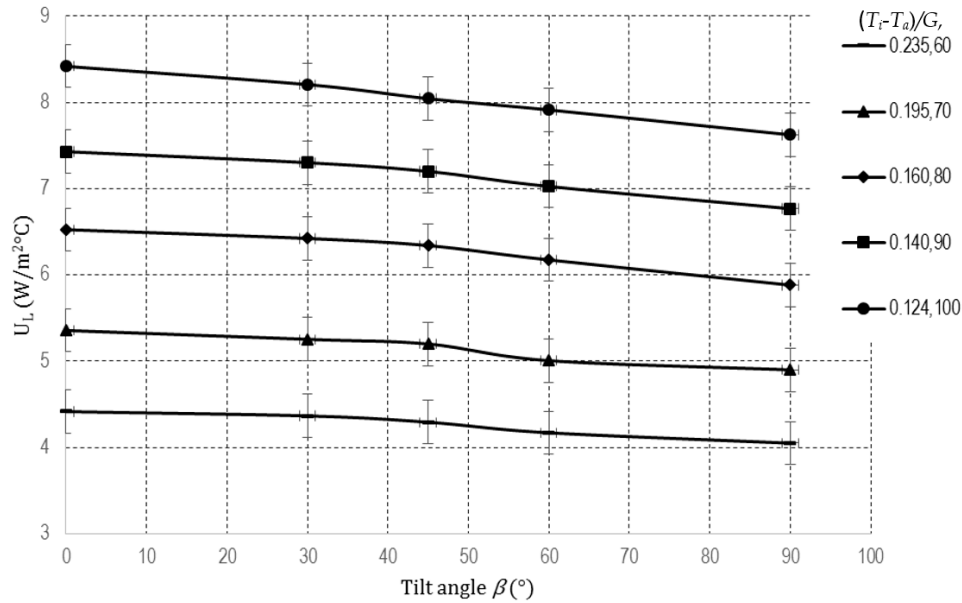**Figure 5.** U_L vs. β, for variable $(T_i - T_a)/G$ at its corresponding T_p, at $Q_u(\beta) = 0$.
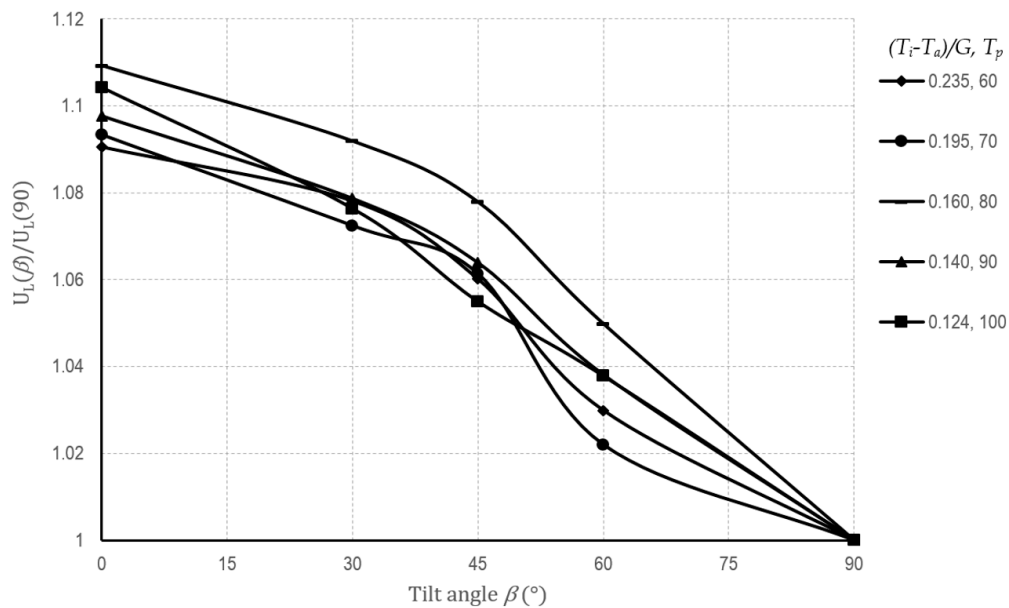

Figure 6. $U_L(\beta)/U_L(90°)$ vs. β and $(T_i - T_a)/G$, at $(T_o - T_i) = 0$.

3.1.3. Comparison with Previous Works

Figure 7 shows a comparison of $U_L(\beta)/U_L(90°)$ vs. β for Case 1 ($Q_u(\beta) > 0$), considering that $U_t \approx U_L$, according Duffie and Beckman [3] and Cooper et al. [8], to calculate U_t. The Hollands correlation [23] was used to calculate the Nussetl number in both methods. Significant changes of $U_L(\beta)/U_L(90°)$ are evident up to 10.0%, comparing different results with different types of collectors and experimental conditions.

According to the uncertainty propagation method [23], in Case 2 the experimental uncertainty of U_L was 0.07 W/m$^2\cdot$°C, which was 247% lower than the value obtained in Case 1. The reduction in uncertainty was reached due to the elimination of $Qu(\beta)$ in Equation (2). The elimination of $Qu(\beta)$ implied that $(T_o - T_i) = 0$, which caused the absorber plate not to have significant temperature changes through the raising tubes. Also, the Joule effect controlled by PID allows us to achieve lower uncertainty, but in Case 1 the greatest contribution of uncertainty continues to be the uncertainty of the mass flow rate.

In Case 1, where the temperature profile of the raising tubes of the collector changes significantly, the U_L is considerably sensitivity to the β and $(T_i - T_a)/G$, reaching up to 19.2% and 41.7%, respectively. The most significant change of $U_L(\beta)/U_L(90°)$ vs. β was 8.0%, while for Case 2, where the raising tubes do not have a significant temperature profile, the maximum change of $U_L(0)/U_L(90°)$ vs. β was only 1.8%. On the other hand, the comparison of the results with different authors showed that there are still considerable differences.
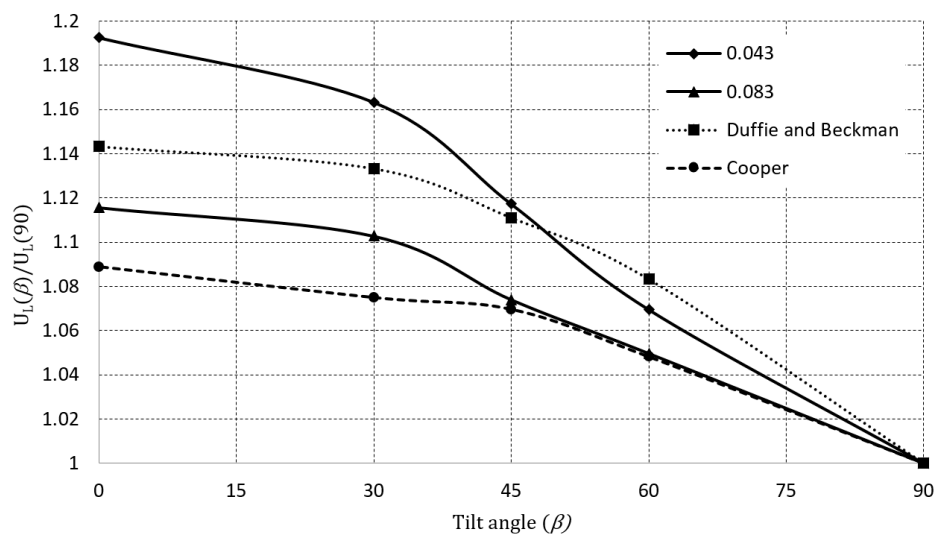

Figure 7. Comparison of $U_L(\beta)/U_L(90°)$ vs. β and $(T_i - T_a)/G$ at $(T_o - T_i) > 0$.

3.2. Efficiency vs. β and $(T_i - T_a)/G$

Figure 8 shows the thermal efficiency η vs. $(T_i - T_a)/G$ at β (0°, 30°, 45°, 60° and 90°). Within the range we studied, the variation of the efficiency with respect to $(T_i - T_a)/G$ reached up to 0.31–0.45 (45%). Similarly, the variation of the efficiency with respect to β reached up to 0.37–0.45 (21.6%). According to the slope of each linear approach, the $F_R U_L(\beta)$ at each inclination angle was 3.12, 3.27, 3.38, 3.52 and 3.65, respectively. These variations behave in almost a linear manner over the inclination range, as in Equation (4), changing 17.6%.

$$F_R U_L(\beta) = 3.112 + 0.0061\beta \tag{4}$$

As expected, the efficiency slowed down as β and $(T_i - T_a)/G$ increased, showing average variations of 21.6% and 45.0%, respectively, over the studied range. According to the least squares fitting method, considering double fitting, the efficiency curve in terms of β and $(T_i - T_a)/G$ is equated in Equation (5). The *RMSE* and R^2 were 0.008 and 0.982, respectively, taking into account the experimental data.

$$\eta\left(\beta, \left[\frac{T_i - T_a}{G}\right]\right) = 0.5282 - 3.386\left[\frac{T_i - T_a}{G}\right] + 0.0008145\beta \tag{5}$$

Equation (5) allows us to observe that the heat transfer convection between the absorber plate and glazing cover is significantly affected by changes of β and $(T_i - T_a)/G$, which in turn significantly affects the accuracy of the overall heat transfer coefficient and the thermal efficiency of the flat plate collectors.
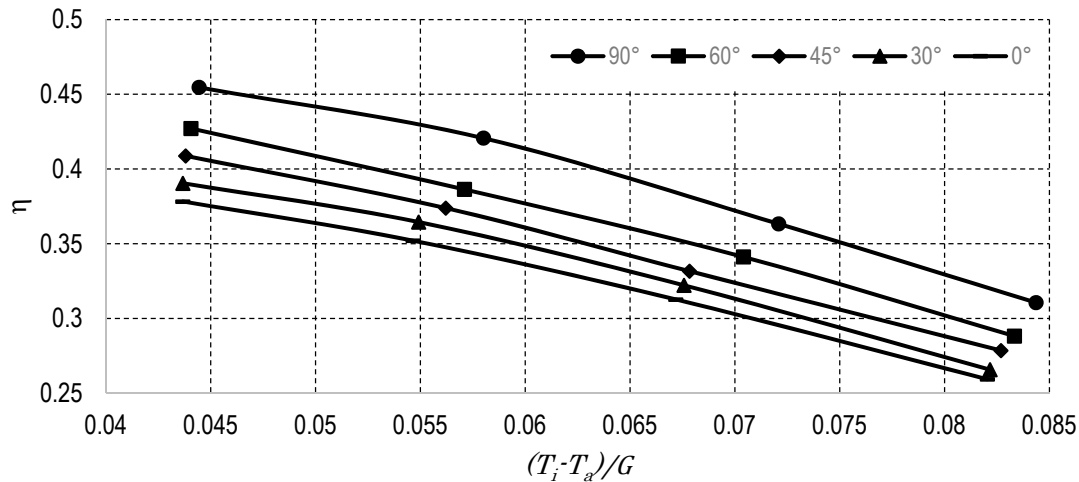

Figure 8. η vs. β and $(T_i - T_a)/G$.

4. Conclusions

The effects of varying the angle of inclination are reflected directly in the overall loss coefficient which in turn significantly affects the thermal efficiency. Within the range we studied, the average variation of the efficiency with respect to β and $(T_i - T_a)/G$ was 21.6% and 45.0%, respectively. At the same time, the U_L is also considerably sensitivity to the β and $(T_i - T_a)/G$, reaching up to 19.2% and 41.7%, respectively. A two-fitting variable correlation was obtained from the efficiency with respect to the $(T_i - T_a)/G$ and β, with *RMSE* and R^2 values of 0.008 and 0.982, respectively.

The most significant changes of $U_L(β)/U_L(90°)$ vs. β were found for Case 1: $(T_o - T_i) > 0$, 8.0%, where the temperature profile of the raising tubes of the collector changes significantly. On the other hand, for Case 2: $(T_o - T_i) = 0$, where the raising tubes do not have a significant temperature profile, the maximum change of $U_L(β)/U_L(90°)$ vs. β was 1.8% only, which is negligible. A critical angle was found between 30°and 45° of the collector's inclination, which is similar for all the values of the $(T_i - T_a)/G$, while the variation between 0°–30° and 45°–90° seems to be almost linear in its behavior.

The $F_R U_L(β)$ varied up to 17.6% from the horizontal to vertical position. These variations behave almost linearly over the inclination range with respect to the average value. Therefore, the effects of the changes of β considerably influence the efficiency calculations of solar collectors if changes of the convective flow patterns within collector are not considered.

Author Contributions: Orlando Montoya-Marquez and José Jasson Flores-Prieto conceived and designed the experiments; Orlando Montoya-Marquez performed the experiments; both authors analyzed the data and contributed reagents/materials/analysis tools; also, Orlando Montoya-Marquez and José Jasson Flores-Prieto wrote the paper.

Nomenclature

Variables	Description	Units
A	Collector area	m^2
Cp	Specific heat	J/kg°C
F_R	Removal factor	-
G	Solar radiation	W/m^2
$\dot{m}$	Mass flow	kg/s
Q_i	Input heat	W
Q_l	Loss heat	W
Qu	Useful heat	W
$RMSE$	Root mean square error	-
R^2	Coefficient of determination	-
T_a	Ambient Temperature	°C
T_i	Input temperature	°C
T_o	Output temperature	°C
T_p	Mean absorber plate temperature	°C
U_L	Overall heat transfer coefficient	W/m^2·°C
VI	Electric power	W
Symbols		
α	Absorptance	-
β	Tilt angle	°
τ	Transmittance	-
η	Efficiency	-
Acronyms		
ASHRAE	American Society of Heating Refrigerating and Air Conditioning Engineers	
ANSI	American National Standard Institute	
IAM	Incident Angle Modifier	
IEA	International Energy Agency	
CIE	Commission Internationale de L´Eclairage	
ISO	International organization for standardization	

References

1. Mauthner, F.; Weiss, W.; Spörk-Dür, M. *Solar Heat Worldwide*; IEA Solar Heating & Cooling Programme: Gleisdorf, Austria, 2016.
2. Kalogirou, S.A. Solar thermal collectors and applications. *Prog. Energy Combust. Sci.* **2004**, *30*, 231–295. [CrossRef]
3. Duffie, J.; Beckman, W. *Solar Engineering of Thermal Processes*, 4th ed.; John Wiley & Sons, Inc.: Hoboken, NJ, USA, 2013.
4. American Society of Heating, Refrigerating, and Air-Conditioning Engineers, Inc. *ANSI/ASHRAE 93-2010 (RA 2014), Methods of Testing to Determine the Thermal Performance of Solar Collectors*; ASHRAE: Atlanta, GA, USA, 2014.
5. *ISO 9806-1 International Standard, Test Methods for Solar Collectors—Part 1: Thermal Performance of Glazed Liquid Heating Collectors Including Pressure Drop*; ISO: Vernier, Switzerland, 1994.
6. Whillier, A. Prediction of performance of Solar Collectors. In *Applications of Solar Energy for Heating and Cooling of Buildings*; ASHRAE GRP 170; ASHRAE: New York, NY, USA, 1977.
7. Cooper, P.I. The effect of inclination on the heat loss from flat-plate solar collectors. *Sol. Energy* **1981**, *27*, 413–420. [CrossRef]
8. Cooper, P.I.; Dunkle, R.V. A non-linear flat plate collector model. *Sol. Energy* **1981**, *26*, 133140. [CrossRef]
9. Rodríguez-Hidalgo, M.C.; Rodríguez-Aumente, P.A.; Lecuona, A.; Gutiérrez-Urueta, G.L.; Ventas, R. Flat plate thermal solar collector efficiency: Transient behavior under working conditions. Part I: Model description and experimental validation. *Appl. Therm. Eng.* **2011**, *31*, 2394–2404. [CrossRef]
10. Chang, T.P. Study on the optimal tilt angle of solar collector according to different radiation types. *Int. J. Appl. Sci. Eng.* **2008**, *6*, 151–161.
11. Shariah, A.; Al-Akhras, M.A.; Al-Omari, I.A. Optimizing the tilt angle of solar collectors. *Renew. Energy* **2002**, *26*, 587–598. [CrossRef]

12. Ozoe, H.; Sayama, H.; Churchill, S.W. Natural convection in an inclined rectangular channel at various aspect ratios and angles—Experimental measurements. *Int. J. Heat Mass Transf.* **1975**, *18*, 1425–1431. [CrossRef]

13. Ozoe, H.; Yamamoto, K.; Sayama, H.; Churchil, S.W. Natural convection in an inclined rectangular channel heated on one side and cooled on the opposing side. *Int. J. Heat Mass Transf.* **1974**, *17*, 1209–1217.

14. Alvarado, R.; Xamán, J.; Hinojosa, J.; Álvarez, G. Interaction between natural convection and surface thermal radiation in tilted slender cavities. *Int. J. Therm. Sci.* **2008**, *47*, 355–368. [CrossRef]

15. Bava, F.; Furbo, S. Correction of Collector Efficiency Depending on Variations of Collector Type, Solar Collector Fluid, Volume Flow Rate and Collector Tilt. IEA-SHC Info Sheet 45.A.1. 22 December 2014. Available online: http://task45.iea-shc.org/data/sites/1/publications/IEA-SHC-T45.A.1-INFO-Correction-of-collector-efficiency.pdf (assessed on 21 December 2016).

16. Sabatelli, V.; Marano, D.; Braccio, G.; Sharma, V.K. Efficiency test of solar collectors: Uncertainty in the estimation of regression parameters and sensitivity analysis. *Energy Convers. Manag.* **2002**, *43*, 2287–2295. [CrossRef]

17. Beikircher, T.; Osgyan, P.; Fischer, S.; Drück, H. Short-term efficiency test procedure for solar thermal collectors based on heat loss measurements without insolation and a novel conversion towards daytime conditions. *Sol. Energy* **2014**, *107*, 653–659. [CrossRef]

18. *Glycols*; Curme, G.O.; Johnston, F., Eds.; Reinhold Publishing Corp.: New York, NY, USA, 1952.

19. *CIE 130-1998, Practical Methods for the Measurement of Reflectance and Transmittance*; Technical Report No. 130; Commission Internationale de L´Eclairage: Vienna, Austria, 1998.

20. *ISO9050-2003 Glass in Building—Determination of Light Transmittance, Solar Direct Transmittance, Total Solar Energy Transmittance, Ultraviolet Transmittance and Related Glazing Factors*; ISO: Vernier, Switzerland, 2003.

21. Zauner, C.; Hengstberger, F.; Hohenauer, W.; Reichl, C.; Simetzberger, A.; Gleiss, G. Methods for medium temperature collector development applied to a CPC collector. *Energy Procedia* **2012**, *30*, 187–197. [CrossRef]

22. Holman, J.P. *Experimental Methods for Engineers*, 8th ed.; McGraw-Hill Book Company: New York, NY, USA, 2012.

23. Hollands, K.G.T.; Unny, T.E.; Raithby, G.D.; Konicek, L. Free convection heat transfer across inclined air layers. *J. Heat Transf.* **1976**, *98*, 189–193. [CrossRef]